Research Article

Mandula Buren*, Yingchun Zhao, Long Chang, Guangpu Zhao, and Yongjun Jian

AC electroosmotic flow of Maxwell fluid in a pH-regulated parallel-plate silica nanochannel

https://doi.org/10.1515/phys-2025-0126
received August 15, 2024; accepted January 07, 2025

Abstract: The surface charge property plays a crucial role in the electrokinetic flow in silica nanochannel in which the surface charge is generated by surface chemical reaction and is dependent on the solution pH. In nanofluidic devices, many of the fluids belong to the viscoelastic fluid class. In this work, we develop theoretical analysis for the effects of the solution pH, background salt concentration, and electric field frequency on an alternating current (AC) electroosmotic flow (EOF) of Maxwell fluid. The results show that the velocity amplitude of AC EOF of Maxwell fluid decreases with the background salt concentration and increases with the relaxation time and the deviation of the solution pH from the isoelectric point (pH = 3.05). The velocity amplitude of Maxwell fluid is greater than that of Newtonian fluid. In particular, the velocity amplitude of Maxwell fluid increases with the electric field frequency, whereas the velocity amplitude of Newtonian fluid remains unaffected by the electric field frequency.

Keywords: electric double layer, AC EOF, functional group, pH-regulated nanochannel, Maxwell fluid, viscoelastic fluid

*** Corresponding author: Mandula Buren,** Mandula Buren, School of Mathematical Science, Inner Mongolia Normal University, Hohhot, 010022, China, e-mail: brmdllyc@163.com
Yingchun Zhao: School of Mathematical Science, Inner Mongolia Normal University, Hohhot, 010022, China, e-mail: Yingchun_1983@126.com
Long Chang: School of Statistics and Mathematics, Inner Mongolia University of Finance and Economics, Hohhot, 010070, China, e-mail: suolunga@163.com
Guangpu Zhao: College of Sciences, Inner Mongolia University of Technology, Hohhot, 010051, China, e-mail: zhaoguangpu105@sina.com
Yongjun Jian: Institute for Nonlinear Science, Donghua University, Shanghai, 201620, China; School of Mathematics and Statistics, Donghua University, Shanghai, 201620, China, e-mail: jianyj@imu.edu.cn

Nomenclature

C_i	concentration of the ith ionic species (mol/m^3),
C_{i0}	bulk concentration of the ith ionic species (mol/m^3),
E	electric field (V m^{-1})
e	elementary charge (C)
F	Faraday constant (C mol^{-1})
h	half channel height (m)
K_-	equilibrium constant (kmol/m^3)
K_+	equilibrium constant (kmol/m^3)$^{-1}$
K	ratio of half channel height to Debye length
N_A	Avogadro's number (mol^{-1})
R	gas constant (J mol^{-1} K^{-1})
Re_ω	oscillating Reynolds number
T	absolute temperature (K)
t_m	relaxation time (s)
U^*	dimensionless velocity amplitude
u	velocity component (m)
ω	frequency of electric field (s^{-1})
y^*	dimensionless coordinates
y	coordinates (m)
z_i	valence of the ith ionic species
λ_D	Debye length (m)
φ^*, φ_s^*	dimensionless electric potential, dimensionless surface potential
τ_{21}	shear stress component (N m^{-2})
η	zero shear rate viscosity (kg m^{-1} s^{-1})
Γ_i	number site density of the ith species (nm^{-2})
Γ_t	total number site density of SiOH molecules (nm^{-2})
φ	electric potential (V)
σ_s	surface charge density (C m^{-2})
ε	fluid permittivity (F m^{-1})
ρ	fluid density (kg m^{-3})

Abbreviations

AC	alternating current
DC	direct current

EDL electric double layer
EOF electroosmotic flow

1 Introduction

Electroosmotic flow (EOF) is the movement of an electrolyte solution in a channel with charged surface under the action of an applied electric field. EOF has many applications such as micropumps, sample separation, and mixers in microfluidics and nanofluidics [1–4]. The charging mechanisms of the wall–fluid interface are complex, possibly including the dissociation or association of functional groups on the wall, the asymmetric dipoles of water molecules residing at the wall–fluid interface and ion adsorption, *etc.* [3]. The presence of surface charges affects the distribution of nearby ions in the electrolyte solution. Counter-ions are attracted toward the charged surface, while co-ions are repelled from the charged surface. These interactions between ions lead to the formation of the so-called electric double layer (EDL) in which the net electric charge density is not zero. Direct current (DC)/alternating current (AC) EOF are generated by a Columbic force which equals the product of the charge density and DC/AC electric field, respectively. AC EOF is also known as time periodic EOF. The problems on the velocity distribution, entropy generation, heat and mass transfers of EOF of Newtonian fluid in nanochannels (with at least one characteristic dimension below or in the order of 100 nm) have been studied extensively [5–12]. Recently, Shit *et al.* [10] investigated the linear stability of a rotating EOF in unconfined and confined configurations by using the Debye–Hückel approximation. In a curved rectangular microchannel [11], the effects of the slip length, the curvature ratio, and the aspect ratio on EOF were studied. Pan *et al.* [12] studied experimentally and numerically EOF and Joule heating in cellular micro/nano electroporation.

In practice, micro- and nanofluidic devices are frequently used to analyze the biofluids (such as blood) and polymer solution (such as polyacrylamide [PAAm] and polyethylene oxide [PEO]) [13–23]. These fluids exhibit non-Newtonian behavior. The blood and PAAm solutions can be described by Maxwell model [13–15] and the simplified Phan–Thien–Tanner (sPTT) model [16], respectively. The solution of cetylpyridinium chloride and sodium salicylate shows linear Maxwell fluid rheology at certain concentrations [14,15]. The ion transport and current rectification of sPTT and Sisko fluid in a conical nanochannels have been studied by Trivedi and Nirmalkar [18] and Tang *et al.* [19], respectively. Koner *et al.* [20] studied AC EOF of Maxwell fluid and mass transport of an electro neutral solute through polyelectrolyte layer-coated canonical nanopore. They also investigated the rheological impact on thermofluidic transport characteristics of fractional Maxwell fluids through a soft nanopore [21]. Siva *et al.* [22] investigated the EOF of couple stress fluid in a rotating microchannel, and found that the increase in the couple stress parameter accelerates the axial EOF inside EDL.

In the previous literature [4–23], it is assumed that the surface charge density remains unaffected by solution properties. However, the surface charge density in nanochannels made of materials like SiO_2 and Al_2O_3 is strongly dependent on hydrogen ions, which means it also depends on the solution pH. Hsu and Huang [24] derived analytical expressions for the electric potential and velocity distributions of EOF in a pH-regulated parallel-plate microchannels. Yeh *et al.* [25] analyzed the effects of the solution pH, bulk ionic concentration, and the applied gate potential on the zeta potential, surface charge density, and velocity of EOF in a charge-regulated parallel-plate nanochannel. They found that the magnitude of surface charge density increases with an increase in pH and the applied gate potential and a decrease in the bulk ionic concentration; the velocity of EOF can be modulated by adjusting the values of the solution pH, bulk ionic concentration and the applied gate potential. Sadeghi *et al.* [26] investigated EOF and ionic conductance in a pH-regulated rectangular nanochannel, and found that the mean velocity first increases with the background salt concentration up to a threshold value of this parameter after which the trend is reversed. Yang *et al.* [27] studied the AC EOF in a pH-regulated parallel-plate nanochannel made of SiO_2. The influences of the number of pH-regulated nanochannels and the distances between adjacent nanochannels on the surface charge density, ionic concentration, and velocity field were investigated [28].

The working fluids in the previous studies [24–28] are all Newtonian fluids in pH-regulated nanochannel. Hsu *et al.* [29], in 2019, studied the non-Newtonian (power law) fluid in a pH-regulated conical nanopore, and analyzed the effects of the solution pH, bulk salt concentration, and the power-law index on the ion transport in the nanopore. Moschopoulos *et al.* [30] conducted a theoretical and experimental investigation on EOF of polyethylene oxide in microchannels, taking into account the deprotonation reaction of silanol groups and the formation of a polymeric depletion layer. Recently, Peng *et al.* [31] in 2024 investigated the effects of electrolyte concentration, pH, and polymer concentration on EOF and ion transport of viscoelastic (Oldroyd-B) fluid in a pH-regulated nanochannel. Mehta *et al.* [32], in 2024, investigated the EOF

characteristics of viscoelastic (PTT) fluid in a pH-regulated parallel-plate microchannel considering the effect of surface charge-dependent slip length.

The experimental and theoretical studies show that there exists fluids which exhibit linear Maxwell fluid rheology at certain concentrations [14,15]. Many researchers have studied EOF of Maxwell fluid and related heat, mass transport problems [13–15,20,33]. However, AC EOF of Maxwell fluid through a pH-regulated nanochannel has not been studied. The aim of the present research is to explore the effects of the solution pH, the background salt concentration, the relaxation time, and the electric field frequency on AC EOF of Maxwell fluid in a parallel-plate silica nanochannel.

2 Mathematical modeling

2.1 Electric potential distribution

We study AC EOF of Maxwell fluid through a slit silica nanochannel separated by $2h$. The channel length and width are assumed to be much larger than the channel height $2h$. The background salt in the fluid is assumed to be KCl. Cartesian coordinate system is placed at the middle of the nanochannel (Figure 1). The functional group SiOH is formed on the channel surface by the reaction between silica and water at wall–fluid interface. The deprotonation and protonation reactions between SiOH and H^+ ions in the fluid give rise to the charged surface, as shown in Figure 1:

$$\mathrm{SiOH} \overset{K_-}{\longleftrightarrow} \mathrm{SiO^-} + \mathrm{H^+}, \quad \mathrm{SiOH} + \mathrm{H^+} \overset{K_+}{\longleftrightarrow} \mathrm{SiOH_2^+}.$$

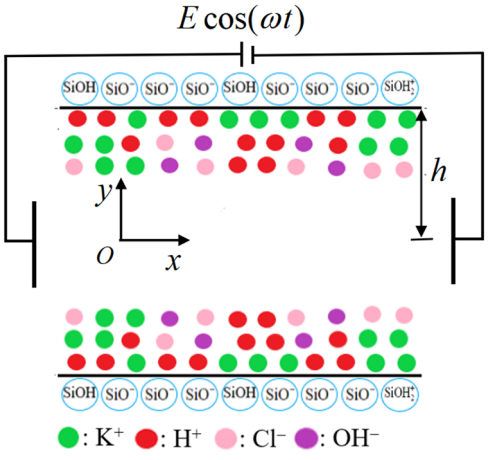

Figure 1: AC EOF in a pH-regulated parallel-plate silica nanochannel subject to an AC electric field along the x-axis.

The equilibrium constants K_- and K_+ of the deprotonation and protonation reactions are equal to

$$K_+ = \frac{\Gamma_{\mathrm{SiOH_2^+}}}{\Gamma_{\mathrm{SiOH}}[\mathrm{H^+}]_s}, \quad K_- = \frac{\Gamma_{\mathrm{SiO^-}}[\mathrm{H^+}]_s}{\Gamma_{\mathrm{SiOH}}},$$

where $\Gamma_{\mathrm{SiO^-}}$, $\Gamma_{\mathrm{SiOH_2^+}}$, and Γ_{SiOH} represent the number site density ($\mathrm{nm^{-2}}$) of $\mathrm{SiO^-}$, $\mathrm{SiOH_2^+}$, and SiOH, respectively; $[\mathrm{H^+}]_s = 10^{-\mathrm{pH}} \exp\left(-\frac{F\phi_s}{RT}\right)$ denotes $\mathrm{H^+}$ ion concentration ($\mathrm{kmol/m^3}$) at the channel surface, in which $10^{-\mathrm{pH}}$, ϕ_s, F, R, and T are the bulk molar concentrations of $\mathrm{H^+}$, the surface electric potential, Faraday constant, gas constant, and the absolute temperature, respectively.

The surface charge density σ_s ($\mathrm{cm^{-2}}$) equals

$$\begin{aligned}\sigma_s &= 10^{18} e(\Gamma_{\mathrm{SiOH_2^+}} - \Gamma_{\mathrm{SiO^-}}) \\ &= -\frac{10^{18} F \Gamma_t}{N_A}\left(\frac{K_- - K_+[\mathrm{H^+}]_s^2}{K_- + [\mathrm{H^+}]_s + K_+[\mathrm{H^+}]_s^2}\right),\end{aligned} \tag{1}$$

where $\Gamma_t = \Gamma_{\mathrm{SiOH_2^+}} + \Gamma_{\mathrm{SiO^-}} + \Gamma_{\mathrm{SiOH}}$; e and N_A are the elementary charge and Avogadro's number, respectively [26].

The relation between σ_s and ϕ_s can be obtained from the overall electroneutrality condition of the ions in the surface and the fluid.

$$\sigma_s = \varepsilon \frac{\mathrm{d}\phi}{\mathrm{d}y}, |_{y=h} \tag{2}$$

where ε is the fluid permittivity and ϕ is the electric potential in EDL [26,27]. The K^+, H^+, Cl^-, and OH^- in an unidirectional flow through a parallel-plate nanochannel obey Boltzmann distributions $C_i = C_{i0} \exp\left(-\frac{z_i F \phi}{RT}\right)$, $i = 1, 2, 3, 4$ with bulk concentration C_{i0} ($\mathrm{mol/m^3}$), respectively. These bulk concentrations satisfy the electroneutrality condition, *i.e.*, $C_{10} + C_{20} = C_{30} + C_{40}$. Here the valences $z_1 = z_2 = -z_3 = -z_4 = 1$, and we assume that $\phi\,|_{y=0} = 0$ [26,27].

When pH ≤ 7, the solution pH is adjusted with HCl, and hence, $C_{10} = M_{\mathrm{KCl}} \times 10^3$, $C_{20} = 10^{-\mathrm{pH}+3}$, $C_{30} = C_{10} + 10^{-\mathrm{pH}+3} - 10^{\mathrm{pH}-14+3}$, and $C_{40} = 10^{\mathrm{pH}-14+3}$. When pH >7, the solution pH is adjusted with KOH, and hence, $C_{10} = C_{30} - 10^{-\mathrm{pH}+3} + 10^{\mathrm{pH}-14+3}$, $C_{20} = 10^{-\mathrm{pH}+3}$, $C_{30} = M_{\mathrm{KCl}} \times 10^3$, and $C_{40} = 10^{\mathrm{pH}-14+3}$. Here M_{KCl} ($\mathrm{kmol/m^3}$) is the molar concentration of KCl [26,27].

The electric potential in EDL satisfies the following equations and boundary conditions [3]:

$$\varepsilon \frac{\mathrm{d}^2\varphi}{\mathrm{d}y^2} = -\rho_e, \tag{3}$$

$$\rho_e = -2FC_0 \sinh\left(\frac{F\varphi}{\mathrm{RT}}\right), \tag{4}$$

$$\varphi\,|_{y=h} = \varphi_s,\ \frac{d\varphi}{dy}\,|_{y=0} = 0, \tag{5}$$

where $C_0 = C_{10} + C_{20} = C_{30} + C_{40}$. φ_s in Eq. (5) can be determined by solving Eq. (1) after substituting Eq. (2) in Eq. (1).

Introducing the following variables:

$$y^* = \frac{y}{h},\ K = \frac{h}{\lambda_D},\ \varphi^* = \frac{\phi}{\phi_0},\ \varphi_0 = \frac{RT}{F},\ \lambda_D = \sqrt{\varepsilon RT/2F^2C_0}, \tag{6}$$

where λ_D is the Debye length, we get the dimensionless Poisson–Boltzmann equation and boundary conditions for electric potential

$$\frac{d^2\varphi^*}{dy^{*2}} = K^2 \sinh(\varphi^*), \tag{7}$$

$$\varphi^*\,|_{y=1} = \varphi_s^*,\ \frac{d\varphi^*}{dy^*}\,|_{y^*=0} = 0. \tag{8}$$

The dimensionless surface potential ϕ_s^* can be obtained by solving the following dimensionless equation using MATLAB function *fzero*:

$$\frac{K_- - K_+[H^+]_s^2}{K_- + [H^+]_s + K_+[H^+]_s^2} = -\frac{2\varepsilon\,\phi_0 K}{\sigma_0 h}\sinh\left(\frac{\phi_s^*}{2}\right), \tag{9}$$

where $[H^+]_s = 10^{-pH}\exp(-\phi_s^*)$, $\sigma_0 = \frac{10^{18}FI_t}{N_A}$. From Eq. (7) and boundary conditions (8), we obtain

$$\phi^*(y^*) = 4\tanh^{-1}\left[\exp(K(y^* - 1))\tanh\left(\frac{\phi_s^*}{4}\right)\right]. \tag{10}$$

2.2 Velocity distribution

In a pH-regulated parallel-plate nanochannel as depicted in Figure 1, an AC EOF of an incompressible viscoelastic fluid is generated along the x-axis by Coulomb forces that act on the net charge density near the wall, under the influence of an AC electric field represented by $E\cos(\omega t)$ in the x-axis. Here ω is frequency and t is time. The viscoelastic fluid is assumed to be Maxwell model. The effect of the induced magnetic field on AC EOF of Maxwell fluid is neglected, as the magnetic Reynolds number $Re_m \ll 1$. Here $Re_m = U_{HS}h/\nu_m$, U_{HS} is Helmholtz–Smoluchowski electroosmotic velocity and ν_m is the magnetic diffusivity [33].

From continuity equation and momentum equation for unidirectional flow of incompressible fluid, we obtain the governing equation for velocity distribution [34].

$$\rho\frac{\partial u}{\partial t} = \frac{\partial}{\partial y}\tau_{21} + \rho_e E\,\cos(\omega t), \tag{11}$$

where $u(y, t)$ is the x-component of the velocity of EOF and ρ is the fluid density. For Maxwell fluid, the shear stress component τ_{21}, which is acting on y-plane in x direction, satisfies the constitutive relation of the Maxwell fluid [34]

$$\tau_{ij} + t_m\frac{\partial}{\partial t}\tau_{ij} = \eta\left(\frac{\partial u_i}{\partial x_j} + \frac{\partial u_j}{\partial x_i}\right), \tag{12}$$

where t_m is called relaxation time or memory span of the Maxwell fluid and η is zero shear rate viscosity. From Eqs. (11) and (12), we obtain

$$\rho\frac{\partial u}{\partial t} + \rho\, t_m\frac{\partial^2 u}{\partial t^2} = \eta\frac{\partial^2 u}{\partial y^2} + \rho_e E\cos\omega t + \rho_e t_m\frac{d}{dt}(E\cos\omega t). \tag{13}$$

Assuming

$$u = \mathrm{Re}\{U(y)e^{i\omega t}\},\ E\cos\omega t = \mathrm{Re}\{Ee^{i\omega t}\}, \tag{14}$$

and substituting these expressions in Eq. (13), we obtain

$$\eta\frac{d^2U}{dy^2} - (i\omega - \omega^2 t_m)\rho U = -\rho_e E(1 + i\omega t_m). \tag{15}$$

Here Re{} is the real part of a complex number, i is the imaginary unit.

Let

$$U^*(y^*) = \frac{U}{U_{eo}},\ U_{eo} = -\frac{\varepsilon ERT}{\eta F},\ \mathrm{Re}_\omega = \frac{h^2\omega\rho}{\eta}, \tag{16}$$

substituting Eqs (4), (6), and (16) in Eq. (15), we obtain

$$\frac{d^2U^*}{dy^{*2}} - (i - t_m\omega)\,\mathrm{Re}_\omega U^* = -(1 + it_m\omega)K^2\sinh(\phi^*). \tag{17}$$

Here Re_ω is the oscillating Reynolds number. The velocity adheres to the non-slip boundary condition due to the hydrophilic nature of the silica surface. Because the silica surface is hydrophilic, the velocity satisfies non-slip boundary condition [27],

$$U^*|_{y=1} = 0,\ \left.\frac{dU^*}{dy^*}\right|_{y=0} = 0. \tag{18}$$

Solving Eq. (17) with boundary conditions (18), the semi-analytical solution for velocity can be obtained as

$$U^*(y^*) = A\,\cosh[\sqrt{(i - t_m\omega)\,\mathrm{Re}_\omega}\,y^*] + \frac{(1 + it_m\omega)K^2}{\sqrt{(i - t_m\omega)\,\mathrm{Re}_\omega}}f(y^*), \tag{19}$$

where

$$f(y^*) = \int_0^{y^*} \sinh[\phi^*(y')] \sinh[\sqrt{(i - t_m\omega)\,\mathrm{Re}_\omega}\,(y' - y^*)]\mathrm{d}y',$$

$$A = \frac{-(1 + \mathrm{i}t_m\omega)K^2}{\sqrt{(i - t_m\omega)\,\mathrm{Re}_\omega}\,\cosh\sqrt{(i - t_m\omega)\,\mathrm{Re}_\omega}} f(1).$$

The function $f(y^*)$ can be calculated numerically using Gauss–Legendre integration [35]. The dimensionless velocity can be obtained by

$$\frac{u}{U_{eo}} = \mathrm{Re}\{U^*(y^*)e^{\mathrm{i}\omega t}\}.$$

When $t_m = 0$ in Eq. (19), the velocity distribution of AC EOF of Newtonian fluid can be obtained [27].

3 Results and discussion

In this section, we analyze the results of the solutions for electric potential and velocity distributions of AC EOF of Maxwell fluid in pH-regulated parallel-plate nanochannel, where the effects of the relaxation time (also known as memory span) t_m, the background salt concentration M_{KCl}, and the solution pH are taken into account. In the following discussion, the values of typical parameters are chosen as per the previous studies [20,24,26,27]: ρ = 1,000 kg m^{-3}, η = 0.001 kg m^{-1} s^{-1}, T = 300 K, R = 8.314 J mol^{-1} K^{-1}, ε = 80 × 8.854 × 10^{-12} F m^{-1}, h = 50 × 10^{-9} m, pK_- = 8, pK_+ = 1.9 (p$K_\pm$ = –log$K_\pm$), Γ_t = 6 nm^{-2}, N_A = 6.22 × 10^{23} mol^{-1}, F = 96485.33 C mol^{-1}. The frequency ω of the external electric field varies from 0 to 10^3 s^{-1}. Consequently, Reynolds number Re_ω varies from 0 to 1 × 10^{-5}. To guarantee the validity of fundamental assumption of undisturbed EDL, the relaxation time t_m should be smaller than $2\pi/\omega$ [33]. Thus, in the following computations, we consider t_m to range from 0 to 10^{-2} s.

The expression of electric potential (10) is similar to the result obtained in the study by Yang *et al.* [27]. When pH = 3.05, the electric potential is zero, and hence the surface charge density is zero (Eq. (2)). Figure 2 shows that the magnitude of surface electric potential in EDL increases with the distance from the pH value to the isoelectric point (pH = 3.05), and decreases with the background salt concentration M_{KCl}. From Figure 2, it can be observed that both the pH and concentration M_{KCl} of the solution have a significant impact on the surface potential.

The effects of t_m and pH on the velocity amplitude of AC EOF at fixed M_{KCl} = 0.002 M and $\omega = 10^2$ Hz are depicted in Figure 3. Comparing these figures, it is found that the velocity amplitude of Maxwell fluid is larger than that of Newtonian fluid (corresponding to t_m = 0); the velocity amplitude of AC EOF of Maxwell fluid increases with the relaxation time t_m. The reason is that an increase in the relaxation time can result in enhanced fluidity. Figure 3(a) and (b) indicate that there is not much difference in the flow fields between Newtonian fluid and Maxwell fluid when t_m is small. The velocity amplitude increases with the distance from the pH value to the isoelectric point (pH = 3.05) due to the increase in surface potential magnitude (Figure 2). The change in pH value of the solution alters the surface potential and net charge density within EDL, thereby modifying the flow field. When pH = 3.05, the

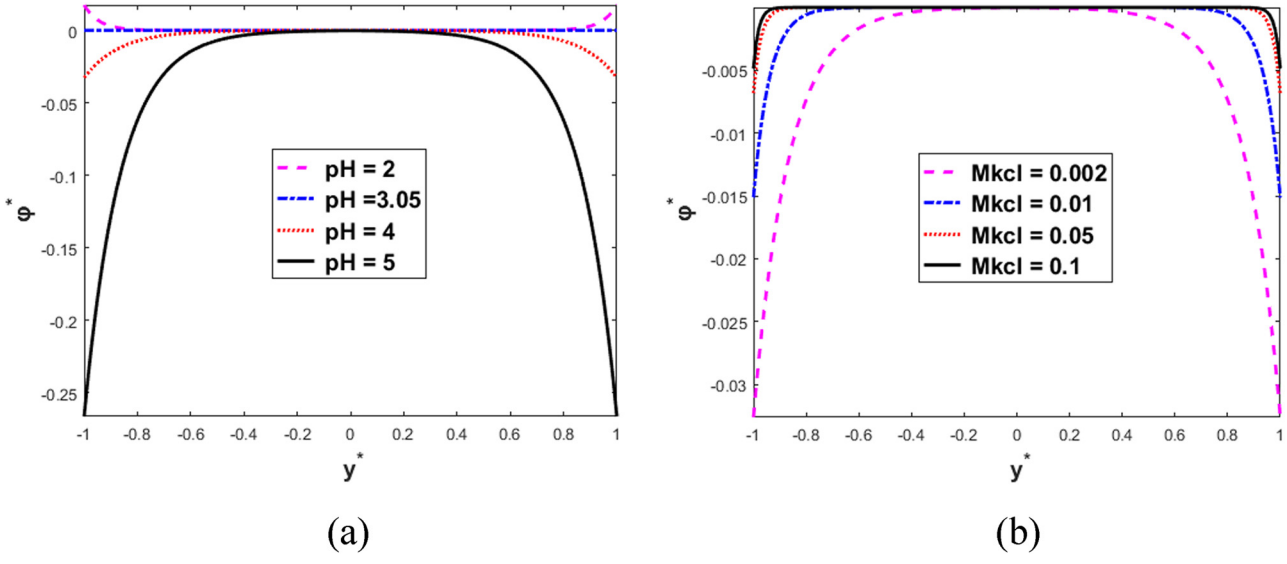

Figure 2: Dimensionless electric potential distributions for different pH and M_{KCl}. (a) M_{KCl} = 0.002 M and (b) pH = 4.

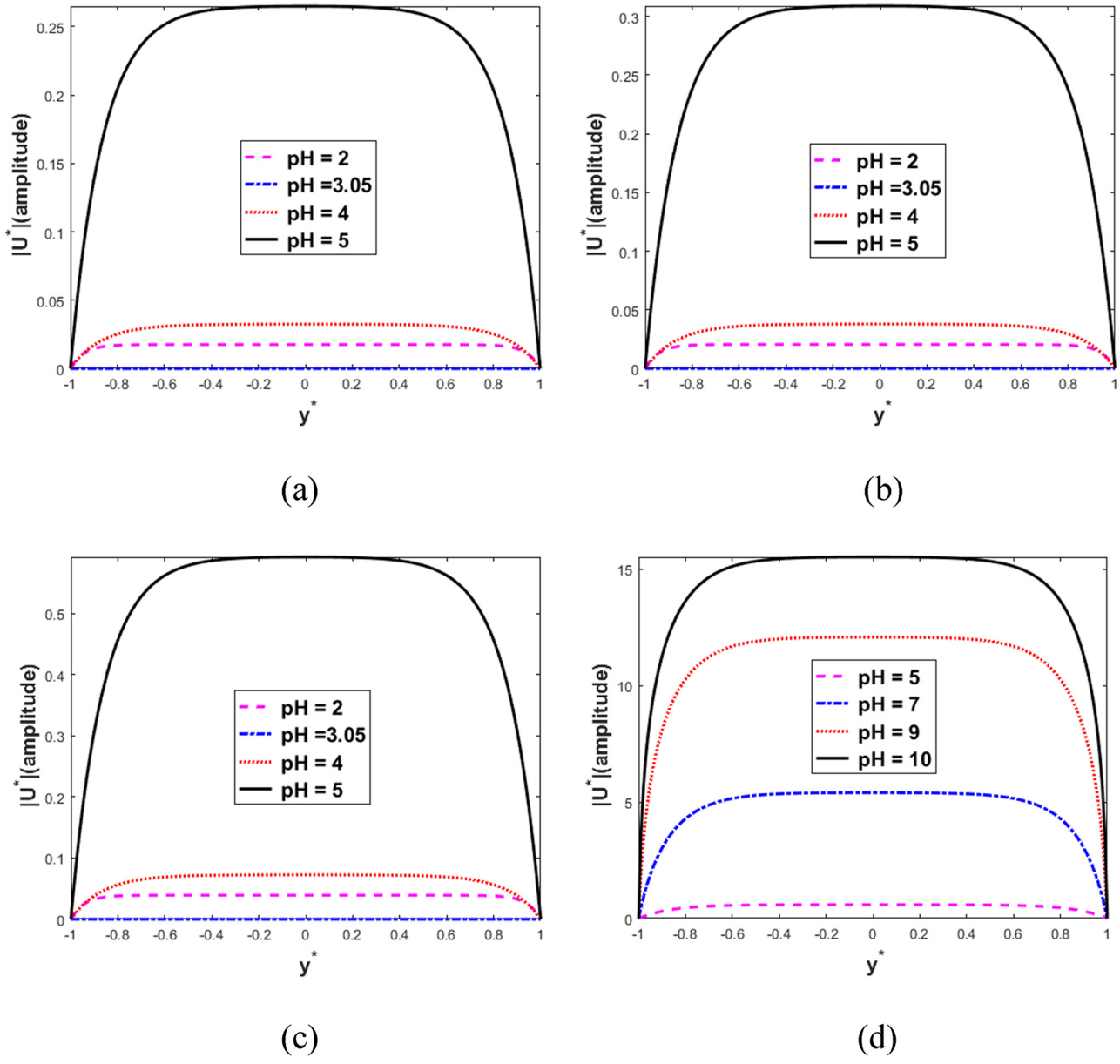

Figure 3: The dimensionless velocity amplitude at M_{KCl} = 0.002 M and $\omega = 10^2$ Hz for different pH and t_m: (a) t_m = 0 s, (b) t_m = 0.006 s, and (c) and (d) t_m = 0.02 s.

surface charge density is zero, and hence EOF is not generated.

Figure 4 depicts the velocity amplitude of AC EOF of Maxwell fluid for different M_{KCl} and t_m when pH = 4 and $\omega = 10^2$ Hz. The velocity amplitude decreases with the increase in M_{KCl}. This is because the surface potential decreases with M_{KCl} (Figure 2). The variations in velocity amplitude of Maxwell fluid with M_{KCl} and pH are similar to that of Newtonian fluid [26,27] (Figures 3 and 4). It also can be seen from Figure 4 that the velocity amplitude increases with the relaxation time t_m. Figure 4(a) and (b) also show that when the relaxation time t_m is small, the difference in the flow fields between Newtonian fluid and Maxwell fluid is small. Figures 2 and 4 illustrate the significant influence of the concentration M_{KCl} on the electric potential and flow field.

Figure 5 shows the effects of the frequency of AC electric field on EOF in the pH-regulated nanochannel. Interestingly, it has been observed that the velocity amplitude of Maxwell fluid increases with an increase in the electric field frequency, while the velocity amplitude of Newtonian fluid remains unaffected by the changes in the electric field

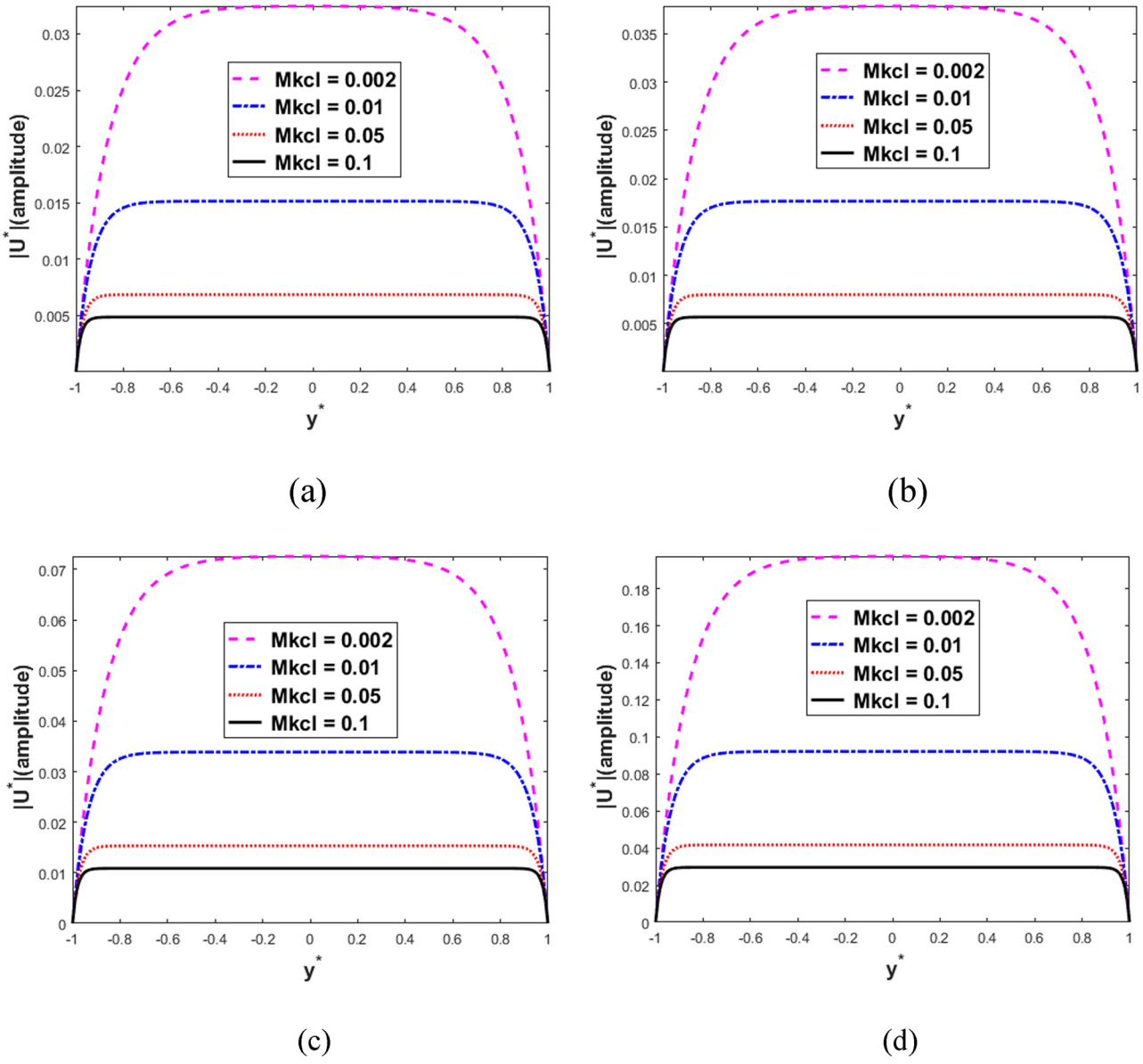

Figure 4: The dimensionless velocity amplitude at pH = 4 and $\omega = 10^2$ Hz for different M_{KCl} and t_m: (a) $t_m = 10^{-4}$ s, (b) $t_m = 0.006$ s, (c) $t_m = 0.02$ s, and (d) $t_m = 0.06$ s.

frequency. The reason is that the term $t_m\omega$ appearing in the governing Eq. (17) of EOF of Maxwell fluid gives rise to the variation in velocity amplitude of Maxwell fluid with the frequency; the term $t_m\omega$ is *zero* when the working fluid is Newtonian fluid. In addition, the velocity amplitude distribution is a plug-like curve. This is because the oscillating Reynolds number in the nanochannel is too low, *i.e.*, the momemtum diffusion time scale is much smaller than the oscillation period, and consequently, the fluid momentum can diffuse from the EDLs into the middle of the channel.

4 Conclusion

In this work, AC EOF of Maxwell fluid in a pH-regulated parallel-plate silica nanochannel has been studied. The analytical and semi-analytical solutions for the electric potential and velocity are obtained, respectively. The effects of the relaxation time, solution pH, salt concentration, and the frequency of AC electric field on EOF have been analyzed. The absolute value of surface electric potential in EDL increases with the distance from the pH

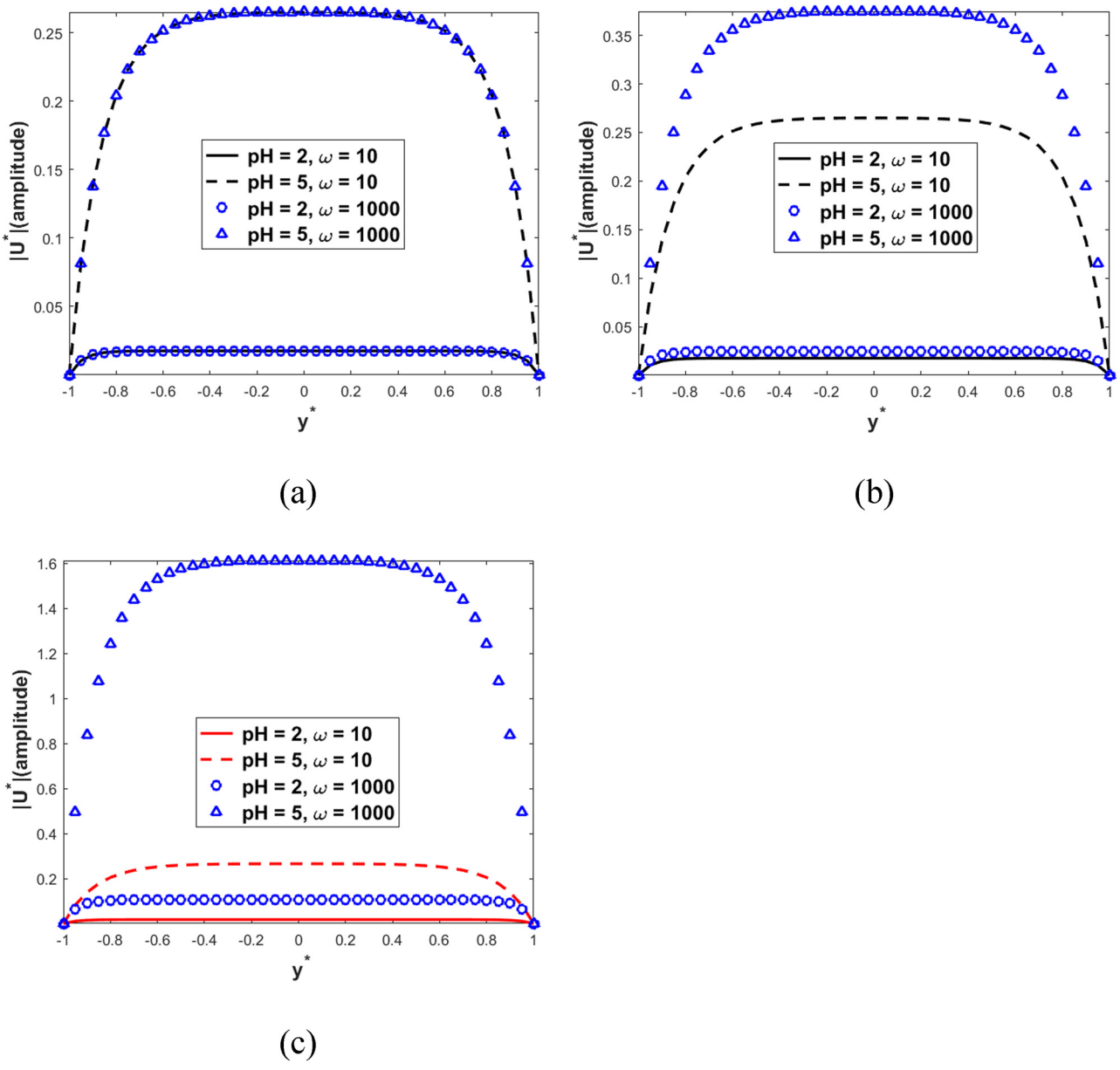

Figure 5: The dimensionless velocity amplitude at M_{KCl} = 0.002 for different pH, ω, and t_m: (a) t_m = 0 s, (b) t_m = 0.001 s, and (c) t_m = 0.006 s.

value to the isoelectric point (pH = 3.05), and decreases with the salt concentration M_{KCl}. The velocity amplitude of AC EOF of Maxwell fluid is larger than that of Newtonian fluid; the velocity amplitude of AC EOF of Maxwell fluid decreases with the salt concentration M_{KCl} and increases with the relaxation time t_m and the distance from the pH value to the isoelectric point (pH = 3.05), respectively. Interestingly, it is observed that the velocity amplitude of Maxwell fluid increases with the increase in electric field frequency ω, while the velocity amplitude of Newtonian fluid remains unaffected by the electric field frequency ω. Interestingly, the velocity amplitude of Maxwell fluid increases with electric field frequency ω, while the velocity amplitude of Newtonian fluid remains unaffected. The electrokinetic flow of the other types of non-Newtonian fluids in pH-regulated channels can be studied in the future.

Funding information: This work was supported by the National Natural Science Foundation of China (Grant No. 12162003), the Innovative Research Team in Universities of Inner Mongolia Autonomous Region (No. NMGIRT2323), the Natural Science Foundation of Inner Mongolia (Grant Nos 2024LHMS01008, 2024LHMS01010, 2023MS01012), the Basic Scientific Research Fund Projects for Directly Affiliated

Universities in the Autonomous Region (No. NCYWT23035), and the Mathematics First-class Disciplines Cultivation Fund of Inner Mongolia Normal University (Grant No. 2024YLKY05).

Author contributions: All authors have accepted responsibility for the entire content of this manuscript and approved its submission.

Conflict of interest: The authors state no conflict of interest.

Data availability statement: All data generated or analyzed during this study are included in this published article.

References

[1] Sun Y, Jiang R, Hu L, Song Y, Li M. Electrokinetic transport phenomena in nanofluidics and their applications. Electrophoresis. 2023;44:1756–73.

[2] Laser DJ, Santiago JG. A review of micropumps. J Micromech Microeng. 2004;14:R35.

[3] Li D. Encyclopedia of microfluidics and nanofluidics. New York: Springer Science & Business Media; 2008.

[4] Lim CY, Lam YC. Analysis on micro-mixing enhancement through a constriction under time periodic electroosmotic flow. Microfluid Nanofluid. 2012;12:127–41.

[5] Haywood DG, Harms ZD, Jacobson SC. Electroosmotic flow in nanofluidic channels. Anal Chem. 2014;86:11174–80.

[6] Silkina EF, Asmolov ES, Vinogradova OI. Electro-osmotic flow in hydrophobic nanochannels. Phys Chem Chem Phys. 2019;21:23036–43.

[7] Conlisk AT, McFerran J, Zheng Z, Hansford D. Mass transfer and flow in electrically charged micro-and nanochannels. Anal Chem. 2002;74:2139–50.

[8] Liu Y, Xing J, Jian Y. Heat transfer and entropy generation analysis of electroosmotic flows in curved rectangular nanochannels considering the influence of steric effects. Int Commun Heat Mass. 2022;139:106501.

[9] Roy D, Bhattacharjee S, De S. Mass transfer of a neutral solute in polyelectrolyte grafted soft nanochannel with porous wall. Electrophoresis. 2020;41:578–87.

[10] Shit GC, Sengupta A, Mondal PK. Stability analysis of electro-osmotic flow in a rotating microchannel. J Fluid Mech. 2024;983:A13.

[11] Liu YB. Effect of boundary slip on electroosmotic flow in a curved rectangular microchannel. Chin Phys B. 2024;33:074101.

[12] Pan J, Wang X, Chiang C, Ma Y, Cheng J, Bertani P, et al. Joule heating and electroosmotic flow in cellular micro/nano electroporation. Lab Chip. 2024;24:819–31.

[13] Bandopadhyay A, Chakraborty S. Electrokinetically induced alterations in dynamic response of viscoelastic fluids in narrow confinements. Phys Rev E. 2012;85:056302.

[14] Lambert AA, Cuevas S, del Río JA, López, de Haro M. Heat transfer enhancement in oscillatory flows of Newtonian and viscoelastic fluids. Int J Heat Mass Tran. 2009;52:5472–8.

[15] Berret JF J, Apell G. Porte, Linear rheology of entangled wormlike micelles. Langmuir. 1993;9:2851.

[16] Mukherjee S, Das SS, Dha J, Chakraborty S, DasGupta S. Electroosmosis of viscoelastic fluids: role of wall depletion layer. Langmuir. 2017;33:12046–55.

[17] Zhao C, Yang C. Electrokinetics of non-Newtonian fluids: A review. Adv Colloid Interf. Sci. 2013;201–202:94–108.

[18] Trivedi M, Nirmalkar N. Ion transport and current rectification in a charged conical nanopore filled with viscoelastic fluids. Sci Rep. 2022;12:2547.

[19] Tang L, Hao Y, Li P, Liu R, Zhou Y, Li J. Ion current rectification properties of non-Newtonian fluids in conical nanochannels. Phys Chem Chem Phys. 2024;26:2895–906.

[20] Koner P, Bera S, Ohshima H. Ion partitioning effects on electrokinetic flow of generalized Maxwell fluids through polyelectrolyte layer coated nanopore under AC electric field. Colloid Polym Sci. 2021;299:1777–95.

[21] Koner P, Bera S, Ohshima H. Rheological impact on thermofluidic transport characteristics of generalized Maxwell fluids through a soft nanopore. Phys Fluids. 2023;35:033612.

[22] Siva T, Kumbhakar B, Jangili S, Mondal PK. Unsteady electro-osmotic flow of couple stress fluid in a rotating microchannel: An analytical solution. Phys Fluids. 2020;32:102013.

[23] Pal SK, Mahapatra P, Ohshima H, Gopmandal PP. Electroosmotic flow modulation and enhanced mixing through a soft nanochannel with patterned wall charge and hydrodynamic slippage. Ind Eng Chem Res. 2024;63:12977–98.

[24] Hsu JP, Huang CH. Analytical expressions for pH-regulated electro-osmotic flow in microchannels. Colloid Surf B. 2012;93:260–2.

[25] Yeh LH, Xue S, Joo SW, Qian S, Hsu JP. Field effect control of surface charge property and electroosmotic flow in nanofluidics. J Phys Chem C. 2012;116:4209–16.

[26] Sadeghi M, Saidi MH, Sadeghi A. Electroosmotic flow and ionic conductance in a pH-regulated rectangular nanochannel. Phys Fluids. 2017;29:062002.

[27] Yang M, Buren M, Chang L, Zhao Y. Time periodic electroosmotic flow in a pH-regulated parallel-plate nanochannel. Phys Scr. 2022;97:030003.

[28] Liu S, Zhang X, Yang Y, Hu N. Ion transport in multi-nanochannels regulated by pH and ion concentration. Anal Chem. 2024;96:5648–57.

[29] Hsu JP, Chu YY, Lin CY, Tseng S. Ion transport in a pH-regulated conical nanopore filled with a power-law fluid. J Colloid Interf Sci. 2019;537:358–65.

[30] Moschopoulos P, Dimakopoulos Y, Tsamopoulos J. Electro-osmotic flow of electrolyte solutions of PEO in microfluidic channels. J Colloid Interf Sci. 2020;563:381–93.

[31] Peng L, Zhang Z, Tang L, Hao Y, Li J. Electrokinetic ion transport of viscoelastic fluids in a pH-regulated nanochannel. Surf Interf. 2024;46:103957.

[32] Mehta SK, Ghosh A, Mondal PK, Wongwises S. Electroosmosis of viscoelastic fluids in pH-sensitive hydrophobic microchannels: Effect of surface charge-dependent slip length. Phys Fluids. 2024;36:023101.

[33] Liu Y, Jian Y, Liu Q, Li F. Alternating current magnetohydrodynamic electroosmotic flow of Maxwell fluids between two micro-parallel plates. J Mol Liq. 2015;211:784–91.

[34] Spurk J, Nuri A. Fluid mechanics. Berlin: Springer; 2008.

[35] Mathews JH, Fink KD. Numerical methods using MATLAB. BeiJing: Publishing House of of Electronics Industry; 2002.